Prepublication version of the paper to appear in:
ASCE Journal of Computing in Civil Engineering

A CELLULAR AUTOMATA MODEL FOR PREDICTING THE FAILURE PATTERN OF LATERALLY LOADED MASONRY WALL PANELS

By G. C. Zhou[1], M.Y. Rafiq[2], G. Bugmann[3], and D. Easterbrook[4]

ABSTRACT: This paper introduces a new technique which directly predicts the failure patterns of laterally loaded masonry panels based on the results of existing typical panels tested in the laboratory. The technique is based on the use of the cellular automata (CA). In this technique, the CA modelling is established to propagate boundary effects to zones within a panel. The corresponding rules for the state values of zones are derived from the proposed CA model, using appropriate transition functions. These state values are then used by the CA to establish zone similarity between two panels. Finally, the zone similarity is applied to establish locations of cracks on the panel. The technique is used in a novel way which eliminates the use of any numerical tools such as finite element analysis (FEA). This technique is purely based on comparing the failure pattern of the base panel (a panel whose failure pattern is known from the laboratory tests) and unseen panels (panels not tested in the laboratory by the authors or their failure pattern are unknown) subjected to the same type of loading and with similar boundary conditions to predict the failure load of the unseen panels.

KEY WORDS: Cellular Automata, Failure Pattern, Masonry Wall Panel, Zone similarity, Base Panel, State Value, Boundary Effect

[1] Zhou, G. C. Professor, Harbin Institute of Technology, Harbin, China.
[2] Rafiq, M. Y., (Corresponding Author) Senior Lecturer, University of Plymouth, School of Engineering, Drake Circus, Plymouth, PL4 8AA, UK. mrafiq@plymouth.ac.uk
[3] Bugmann, G. Reader, University of Plymouth, School of Computing Drake Circus, Plymouth, PL4 8AA, UK gbugmann@plymouth.ac.uk
[4] Easterbrook, D. J., Senior Lecturer, University of Plymouth, School of Engineering, Drake Circus, Plymouth, PL4 8AA, UK. deasterbrook@plymouth.ac.uk

INTRODUCTION

Research on masonry panels subject to lateral loading has focused on searching for accurate and reliable analytical techniques to predict failure loads and failure patterns for the designer. Past research has resulted in a number of techniques such as the yield line theory (British Standard BS5628 2002), the strip method (the Australia code of practice "CSAA" 1969) and finite element analysis (FEA) methods (Baker 1982; Chong 1993; Lee et al. 1996 and Lourenco 1997 & 2000). Lourenco (1997, 2000) proposed an anisotropic softening model which was implemented in DIANA a commercial FEA package. In this model Lourenco derived a material model for masonry which introduces an additional parameter "the fracture energy", besides the tensile strength and flexural rigidity, for evaluating the failure load, failure pattern and deflection of the masonry panels. For validation purposes, Lourenco's applied his model to a number of panels from various sources and the predicted failure load, failure pattern and the load deflection curve for the node with maximum deflection was compared with the laboratory test results of these panels. Although good correlation was achieved for most cases, the failure load at the ultimate load level, which according to Lourenco (1997), is when a fully developed crack occurs at this stage, was underestimated for all panel tested in the University of Plymouth. Beside this Lourenco used modified material properties for these panels which he claimed were "obtained by inverse fitting".

Although Lourenco's model is one of the best models currently available, there are a number of shortcomings that restricts its use in practice:

1. It has been implemented in software mainly used in research in the universities and it is not widely available commercially.
2. The material model has only been incorporated in one commercial package, DIANA, which makes its use restricted in practice.
3. Comparison of load deflection curves has been carried out only for a single point on the panel using the maximum deflection as being representative of the whole panel. This does not model the behaviour of the panel as a whole.
4. Similar to conventional FEA model, Lourenco uses smeared material properties, which does not model variation in the geometric and material properties, which is inherent to masonry panels.

FEA techniques, although widely used in practice, do not always produce accurate predictions of failure loads and failure patterns of masonry panels (Fried 1989; Chong 1993), because the fundamental assumptions on which these theories are based are not fully applicable to masonry panels and accurate modelling of masonry as a brittle and highly composite material, is very difficult. In addition, the two most important factors affecting the behaviour of masonry panels: boundary conditions (West and Webb 1971; West et al. 1971) and variation in masonry properties within the panel (Fried 1989; Lawrence and Lu 1991) have not been modelled properly. Research carried out by the authors, for the first time, has addressed both these issues.

One method of achieving better correlation between predicted response and measured response is the use of model updating techniques. Robert-Nicoud et al. (2005) stated that methods that aim to compute the values of finite-element model parameters through matching predicted responses with measured values are called finite-element model updating or model calibration methods. A comprehensive literature review of various model updating methods is also presented in Robert-Nicoud et al.'s paper.

Friswell and Mottershead (1995) provide a survey of model updating procedures in structural damage detection research, using vibration measurements. Recent papers published in this area include Brownjohn et al.(2003), Castello et al. (2002), Teughels et al. (2002), Modak et al. (2002), Hemez and Doebling (2001), Sohn and Law (2001), Hu et al. (2001). The majority of the research on model updating process involves computing sets of stiffness coefficients that help predict observed vibration modes of structures. The location and extent of damage are inferred through a comparison between the stiffness coefficients of damaged and undamaged structures.

Zhou (2002) developed the concept of stiffness/strength correctors as means of predicting the failure load and failure pattern of laterally loaded masonry panels.

Another novelty of the method developed by Zhou and his co-researcher was that they used only a single panel that was tested in the laboratory and called this "the base panel". They then used cellular automata (CA) to find similar regions called "zones", based on their location from similar boundaries, on any unseen panel; and they derived values of the stiffness/strength correctors for these zones on the unseen panels from a single base panel (see Fig. 1 for details of panel SB01 which is divided into zones. Note that similar zones are shown with the same shades).

{Insert Figure 1 here}

THE CONCEPT OF CORRECTORS AND ZONE SIMILARITY

Zhou (2002) and Rafiq et al. (2003), developed a numerical model that predicts the failure load and failure pattern of masonry wall panels subjected to lateral loading. In this research Zhou and his co-researcher introduced the concept of stiffness/strength correctors which assigns different values of flexural rigidity or tensile strength to various zones within a wall panel. Stiffness/strength correctors values were defined from the comparison of laboratory measured displacement with the finite element analysis computed values of displacement at various locations within the panel.

Zhou and his co-researcher used a number of experimental panels with different geometric properties aspect ratios, and panels with and without openings, for which the stiffness correctors were determined. It was discovered from a comparison of the contour plots of corrector values on these panels, that there appeared to be regions, termed "zones"**,** with similar patterns of corrector values which are closely related to their positions on the panel from similar boundary types. In other words, zones within two panels appear to have almost identical corrector values if these zones are surrounded by similar boundary types.

Based on this finding, Zhou and his co-researchers developed methodologies for establishing zone similarities. In order to obtain a more reasonable and automatic technique for establishing this zone similarity between the base panel and any new (unseen) panel, a cellular automata model was developed to propagate the effect of panel boundaries on zones within the panel and then identify similar zones in two panels. Zhou and his co-researchers, used the CA model, for the first time, to quantify the boundary effect by producing numerical patterns called "state values" for both the base panel and the new panel. Based on these numerical patterns a criterion for matching similar zones between the base panel and the new panel was established.

This technique of zone similarity was mainly based on the concept of finding two similar zones one on the base panel (a panel tested in the laboratory for which displacement values at various load levels at a number of locations on the panel is measured and the failure load and failure pattern for this panel was recorded from a controlled laboratory experiment), and one on the unseen panel (a panel not tested in the laboratory) which are surrounded by similar boundary types and having similar distances from these boundary types. Obviously the exact match is always not possible. Therefore to find a good match for a zone on an unseen panel with a zone on the base panel, the zone on the new panel is

compared with every zone on the base panel and an error value between the state value of the zone in the new panel and the zones on the base panel is calculated. The zone on the base panel with minimum error value is selected as the closest similar zone for the unseen panel. For details of zone similarity techniques please refer to Zhou et al. (2003).

This paper extends that research reported by Zhou (2002), Rafiq et al. (2003) and Zhou et al. (2003) to use the CA to directly predict the failure patterns of solid masonry wall panels. This technique applies the CA "state values" and the criteria for matching similar zones to predict the cracking patterns of new panels based on matching them with the cracking patterns of similar zones on the base panels, for which the failure pattern is known from laboratory experiments. In this process if a zone within the base panel is cracked, its similar zone within the new panel is also assumed to have cracked.

MODELLING PANEL BOUNDARY EFFECTS USING CELLULAR AUTOMATA

Cellular Automata

Cellular Automata (CA) are described as discrete space-time models that consist of cells in a lattice network (Edward 1989). The "neighbourhood" consists of adjacent cells which will influence the behaviour of a particular cell state (Soschinske 1997). Cellular automata provide a framework for a large class of discrete models with homogeneous interactions. The fundamental characteristics of the CA are listed as follows (http://www.tu-bs.de):

1. They consist of a regular discrete lattice of cells.
2. The evolution takes place in discrete time steps.
3. Each cell is characterised by a state taken from a finite set of states.
4. Each cell evolves according to the same rule which depends only on the state of the cell and influenced by the states of a finite number of neighboring cells.
5. The neighborhood relation is local and uniform.

Fig. 2 shows an example of a 2-D neighbourhood cell model developed by von Neumann (Soschinske 1997) and utilised in this paper.

[Insert Figure 2 here]

Halpern et al. (1989) formalised the cellular automata transition model in the case of the von Neumann neighbourhood as:

$$a_{i,j}^{(t+1)} = f(a_{i,j}^{(t)}, a_{i,j+1}^{(t)}, a_{i+1,j}^{(t)}, a_{i,j-1}^{(t)}, a^{(t)}{}_{i-1,j}) \quad (1)$$

where

a = cell state value at a given time interval t
i, j = x, y cell coordinates
t = time interval
f = transition function describing iteration rule

The change in the state value of a cell from time t to time $t+1$ is governed by some "local rules" (Edward 1989) or "transition rules" (Goles et al. 1990). For the CA, neighbourhood structures and transition rules need to be the same for all sites, but not necessarily to be fixed. Updating the state values of the cells for a CA network must be performed by a "synchronous" or parallel mode (Fishburn 1961). Rucker and Rudy (1989) summarised the properties of the CA as follows:

- Parallel: an individual cell is updated independent of other cells;
- Locality: the new cell state value depends on its old cell state value, and the values of its neighbourhood cells at a given time t;
- Homogeneity: the same rules are applied to all cells.

Modelling the Boundary Effect

Zhou (2002) and Rafiq et al (2003) show that zone similarity between a base panel and unseen panels of similar properties are closely related to the panel boundary conditions and the location of each zone relative to the specific panel boundary types. When compared with the properties of, parallel, locality and homogeneity, of the CA, the characteristics of zone similarity can be suitably described by these space properties of the CA. Fig. 3 shows how a panel is modelled using the CA:

[Insert Figure 3 here]

- A panel is divided into a number of zones (cells in a CA system). Initial input values of the transition functions, which are defined in Eqn (2) below, is assigned to each boundary type. In order to achieve better results for matching similar zones, a parametric study was conducted by changing the initial values of each boundary parameter and studying its effect on the Equation (7). The result of this investigation showed that the following initial values were giving the best results for different boundary types: 0.0 for a free edge, 0.2 for a simply supported boundary and 0.4 for a built-in support. For more details of selecting these initial values, refer to Zhou (2002) and Zhou et al. (2003).

- The position of each cell in the CA system corresponds to the position of a zone within the panel.
- Each cell (zone) receives the boundary effect from its neighbourhood cells and in turn propagates the boundary effect to their neighbourhood cells. For a two-dimensional panel, the von Neumann model was found to be sufficient for describing the effect of different boundaries from four supports at the edges of the panel. Therefore, the transition functions of the CA, which are defined in Eqn (2), fully propagate the effect of panel boundaries to individual zones within the panel.

$$\begin{aligned} L_{i,j} &= L_{i,j-1} + \eta\,(1 - L_{i,j-1}) \quad (i = 1, 2,..., M;\ j = 1, 2,..., N) \\ R_{i,j} &= R_{i,j+1} + \eta\,(1 - R_{i,j+1}) \quad (i = 1, 2,..., M;\ j = N, N\text{-}1,..., 2, 1) \\ B_{i,j} &= B_{i+1,j} + \eta\,(1 - B_{i+1,j}) \quad (i = M, M\text{-}1,...,2, 1;\ j = 1, 2,..., N) \\ T_{i,j} &= T_{i-1,j} + \eta\,(1 - T_{i-1,j}) \quad (i = 1, 2,..., M;\ j = 1, 2,..., M) \end{aligned} \tag{2}$$

where

M and N are the numbers of rows and columns of divided zones.

η is the coefficient of transition.

L, R, B and T are the state values of the zones (cells) which are obtained from the propagation of the collective effect from the left, right, bottom and top boundaries respectively.

$L_{i,0}$, $R_{i,N+1}$, $B_{M+1,j}$ and $T_{0,j}$ are the input initial values for the transition functions $L_{i,j}$, $R_{i,j}$, $B_{i,j}$ and $T_{i,j}$. These initial values describe different boundary types identified by specific values.

- The 'state value' $S_{i,j}$ of every zone within the panel is calculated as the average effect from its four adjacent cells, see Eqn (3), which shows that the state value for each cell is closely related to its four neighbourhoods.

$$S_{i,j} = \frac{(L_{i,j} + R_{i,j} + B_{i,j} + T_{i,j})}{4} \quad (i = 1, 2, ..., M,\ j = 1, 2, ..., N) \tag{3}$$

The above proposed CA modelling of boundary effects on zones within the panel reflects the properties of parallel, locality and homogeneity of the CA.

For the property of parallel: the state values of individual cells can be updated independent of other cells/zones to assign unique values to each zone using Eqns (2) and (3). For the property of locality: the new cell/zone state value depends on the state values of its neighbouring cells/zones. For the property of homogeneity: the same rules, Eqns (2) and (3), are applied to all cells/zones within the panel to

calculate a state value for each cell. These state values will then be used to establish zone similarities between zones in a base panel and a new panel

Criterion for Matching Zone Similarity

The cellular automata uses Eqns (2) and (3) to propagate boundary effects to cells/zones within a panel and hence calculate a state value for each cell/zone in a panel based on the distance of each cell/zone from the panel boundaries. The idea for calculating the state values for each cell was to use these state values to find zones within the base panel and unseen panel which are similar and the similarity was determined based on the similar boundary types surrounding the zones.

After some investigation it became clear that comparing the state values of zones was not enough to completely describe zone similarity. In other words, if two zones have the same state value, calculated by Eqns (2) and (3), these two zones do not necessarily have the same corrector. For example, consider a hypothetical panel which is the same as Panel SB01, shown in Fig. 1, except that the right edge support is a built-in support instead of a simply supported support type, which was the case for SB01. The state values of the individual zones are calculated using Eqns (2) and (3) and the result of the CA is summarised in Table 1. In Table 1, Zone D2 has similar state value to zones A5, D3, B7, B3 and C9), but these zones are not similar zones because these zones violate the boundary similarity criteria which is essential for zone similarity (explained in the following section). For example, zone D2 lies close to a fixed edge and zone A5 is adjacent to a free edge, therefore these two zone can not be considered to be similar. Hence it is necessary to define zone similarity by comparing the state value of the cell itself and the state values of its neighbouring cells and the criterion for matching zone similarity between panels is further examined in the following section.

[Insert Table 1 here]

Process Matching Similar Zones

The concept of zone similarity identifies zones for two panels, which are governed by similar boundary types. For this purpose, a criterion needs to be established to match similar zones between a new panel (unseen panel) and a base panel (the correctors are known) based on the concept of zone similarity. The general criterion for matching zone similarity in the above CA model can be defined as:

Firstly, using Eqns (4) and (5) (a general form of equations (2) and (3)), calculate state values for all zones within the new panel and the base panel:

$$\left\{S_i^{new}\right\} = \left\{f(B_l, B_r, B_b, B_t; d_{li}, d_{ri}, d_{bi}, d_{ti})\right\} \quad (4)$$

$$\left\{S_k^{base}\right\} = \left\{f(B_l^{'}, B_r^{'}, B_b^{'}, B_t^{'}; d_{lk}^{'}, d_{rk}^{'}, d_{bk}^{'}, d_{tk}^{'})\right\} \quad (5)$$

where

f is the transition function relationship.

$\left\{S_i^{new}\right\}$ is the vector of state values related to zone i on the new (unseen) panel. This vector includes the state values of the zone i and its four neighbouring zones.

$\left\{S_k^{base}\right\}$ is the vector of state values related to zone k on the base panel. This vector includes the state values of the zone k and its four neighbouring zones.

B_l, B_r, B_b, B_t are parameters identifying boundary type at the left, right, bottom and top edge of the new (unseen) panel respectively.

$B_l^{'}, B_r^{'}, B_b^{'}, B_t^{'}$ are parameters identifying boundary type at the left, right, bottom and top edge of the base panel separately.

$d_{li}, d_{ri}, d_{bi}, d_{ti\,i}$ are the distances from the centre of the zone i to the left, right, bottom and top edges of the new (unseen) panel respectively.

$d_{lk}^{'}, d_{rk}^{'}, d_{bk}^{'}, d_{tk}^{'}$ are the distances from the centre of the zone k to the left, right, bottom and top edges of the base panel respectively.

Secondly, equation (6) is used to establish zone similarity between panels

$$S_Z_j = \underset{k=1}{\overset{MN}{COMPARISON}}\left(\left\{S_i^{new}\right\}, \left\{S_k^{base}\right\}\right) \quad (6)$$

where

S_Z_j is the zone j on the base panel, which is similar to a zone i on a new panel.

$MN = M \times N$ is the total number of zones on the base panel. M and N represent the numbers of zones in row and column within the base panel;

COMPARISON is the criterion for matching similar zones between a base panel and a new panel.

For laterally loaded masonry wall panels, the Eqns (2) and (3) are proposed as the specific expression of the general Eqns (4) and (5), and the Eqn (7), shown below, is proposed as the specific expression of the general Eqn (6)

$$E_{i,j\to new}^{k,l\to base} = \underset{m=1,n=1}{\overset{M,N}{MIN}}\left(\left|S_{i,j}^{new} - S_{m,n}^{base}\right| + \left|S_{i,j-1}^{new} - S_{m,n-1}^{base}\right| + \left|S_{i,j+1}^{new} - S_{m,n+1}^{base}\right| + \left|S_{i-1,j}^{new} - S_{m-1,n}^{base}\right| + \left|S_{i+1,j}^{new} - S_{m+1,n}^{base}\right|\right) \quad (7)$$

where

$E_{i,j\to new}^{k,l\to base}$ is the minimum error of $M \times N$ errors in Eqn. (7). m and n represent the position of a zone on the base panel; i and j represent the position of a zone on the new panel.

Eqn (7) is used to compare the state value of a zone itself and its four neighbourhoods in the new panel with every zone and its four neighbourhood zones on the base panel. An error value is calculated for

each zone by Eqn (7). The zone with the minimum error value on the base panel is defined as the sole similar zone to the zone on the new panel.

In order to assess whether Equation (7) can accurately locate similar zones within a panel, it is necessary to verify its validity. To do this the best test would be to apply this rule to the base panel SB01 and check if this rule can perfectly match similar zones on both sides of the line of symmetry.

The base panel SB01 (Figure 1) was divided into thirty-six zones based on the experimental measured points A1 – A9, B1 –B9, C1 – C9 and D1 – D9. Considering the symmetry of the panel along the vertical central line, there are only 20 different zones on the panel. For instance, Zone D2 is similar to itself and Zone D8. To explain this point better, Figures 4 (a) and (b) show the state values of Zone D2 and its identical symmetrical zone D8 along with their four neighbourhoods with one difference that the state value of the neighbourhood zone on the right of Zone D2 is the same as that of the zone on the left of Zone D8. Therefore, in order to calculate the minimum error using Equation (7) the order of zones on the left and right hand sides of Zone D8 must be reversed.

{Insert Figure 4 here}

To achieve an appropriate matching of similar zones the orientations of the four neighbouring zones were essential in matching similar zones within a panel. It was discovered that considering a fixed orientation for zones within the base panel, each zone within a new panel has eight possible orientations that match the boundaries of the base panel (four facing the front of the panel and four facing the back of the panel. These eight possible orientations are shown in Figures 5 (a) and (b).) Thus, for a zone and its four neighbourhood zones on the new panel, and every zone and its four neighbourhoods on the base panel, Equation (7) is repeatedly used to calculate the errors of the state values of the corresponding zones for eight different orientations for zones on the new panel. The zone on the base panel with the minimum error can be selected to be the similar zone on the new panel.

In the following section techniques described by Zhou and his co-researchers to predict the failure load and failure pattern of masonry wall panels using the CA model is extended to introduce new methodologies that, by matching the failure pattern of the base panel, it is possible to directly predict the failure pattern of a new panel.

{insert Figure 5 here}

PREDICTING FAILURE PATTERNS OF LATERALLY LOADED PANELS DIRECTELY USING CA

Past research has proved that panel boundary types, aspect ratios and dimensions have a significant effect on the failure pattern of a panel (West and Webb 1971; West et al. 1971; Fried 1989). For the existing British Standard (BS5628 2002), the assumption of the shape of the failure pattern is mainly based on the yield line theory and on results obtained from a number of experiments of standard panels. The relationship between the failure pattern and the aspect ratio and boundary types is established empirically. This relationship, reflected in BS 5628, indicates that the failure pattern is related to the behaviour of each zone (cracking or uncracking) on the panel and the behaviour of each zone is related to the aspect ratio and boundary types of the panel. This has been included in the CA modelling of the boundary effects on zones within the panel and the criteria for matching zone similarity described in the previous section. In this study, the CA model of the panel, which is described by the Eqns (2) and (3), and the criteria for matching zone similarity is used to directly (without using FEA) match the failure pattern of the base panel to new panels using (Eqn (7)), in order to produce an intelligent pattern matching technique for predicting the failure pattern for the design of unseen panels. This process can be summarised as follows:

1. The failure pattern on the CA zone/cell mesh of the base panel is based on the failure pattern observed in the laboratory
2. The new/unseen panel is also divided into zones/cells to match the base panel. As stated earlier, zone similarity is determined by the position of zones from similar boundaries therefore, zone dimensions on the new panel should be the same in size or close to those of the base panel (i.e. if the new panel width is half the width of the base panel there would be half as many cells of the same dimension in the new panel as there are in the base panel.)
3. Eqns (2) and (3) are used to calculate the state values of all zones/cells within the base panel and the new/unseen panels.
4. Each zone on the new panel is matched with its similar zone on the base panel using the zone similarity rule Eqn (7).
5. The positions of the cracks on zones within the base panel are established from the laboratory records. This crack pattern is matched on the new panel: (i) locate a cracked zone on the base panel; (ii) match zones which are similar to this zone on the new panel, using zone similarity rules

using equation (7); (iii) the failure pattern on these zones in the new panel is matched with the failure pattern of the base panel (i.e. if there is a crack on a zone in the base there should be a crack on its similar zone on the new panel.

The following case studies examine the validity of the above process on various unseen panels.

CASE STUDIES

In this section a number of laterally loaded unseen wall panels are used to examine the validity of the process introduced in this paper. Panels SB01 and SB06 are full scale panels tested by Chong (1993) in the University of Plymouth. All other panels used in this paper were tested by Lawrence (1983) at the University of South Wales Australia. Only limited information (panel dimension and failure pattern) on these panels was available and details of test results on and material used were not available to the authors.

Details of panels used in these cases studies are summarised in Table 2.

{Insert Table 2 here}

Choice of Base Panels

The boundary conditions of masonry panels in the design standards can be grouped into two main types: (1) four sides constrained; (2) three sides constrained and the fourth side free. Therefore, panels used in the following case studies mainly relate to these panel types.

Three panels that were tested in the laboratory (SB01 and SB05 tested by Chong (1993) in the University of Plymouth and Test panel 29, tested by Lawrence (1983) in the University of South Wales Australia) were used as the base panels for predicting the failure pattern on panels with three sides constrained. It is worthwhile to note that panel SB05 had a damp proof course (dpc) at it base while panels SB01 and Test 29 were not supported on a dpc. The configuration and failure pattern of the base panel was noted from the experimental records of Panels (SB01, SB05 with dpc (Chong 1993) and Test 29 (Lawrence 1983)), as shown in Fig. 6. All these panels have the similar boundary types, e.g., a free top edge and the two vertical edges are simply supported. The bottom edges of Panels SB01 and SB05 are built-in and that of Panel Test 29 is simply supported. Because the supports of the three panels are symmetrical about their central vertical lines, their failure patterns are logically expected to be also symmetrical about the central vertical lines. The panel SB05 is considered to have a symmetrical

failure pattern, therefore this panel was selected as the base panel for all panels with three sides restrained and panels SB01 and Test 29 were ignored.

Similarly, for panels with 4 sides simply supported panel Test 24, tested by Lawrence (1983) was used as the base panel.

Case study 1: Test Panel 21

Fig. 7(a) shows the experimental failure pattern of a single leaf brick panel, Test 21 (Lawrence 1983) with the size 3750mm x 2500 mm x 109mm and three simply supported edges and the top free edge. It is worthwhile to note that the length of this panel is smaller than the base panel (Panel SB05). Fig. 7(c) shows the failure pattern of the base panel (Panel SB05) using the CA zone/cell mesh. Fig. 7(b) shows the failure pattern of the Panel Test 21, predicted by the CA by matching the cracked pattern of similar zones on the base panel (SB05) using the zone similarity concept, Eqn (7). Comparing Figs. 7(a) and 7(b), the predicted failure pattern of the panel Test 21 is very similar to the real cracking pattern of this panel.

[Insert Figure 6 here]

[Insert Figure 7 here]

Case study 2: Test Panel 16

This panel was also tested by Lawrence (1983). Once again, the panel SB05, in the last example, is used as the base panel. The size of this panel is the same as Test Panel 21, discussed in the previous example. Fig. 8 shows the predicted failure pattern of the Test Panel 16 using the proposed CA method. Once again the failure pattern predicted by the CA is very close to that of the experimental result. It can be concluded that the proposed method was able to reasonably predict the failure pattern of both panels.

[Insert Figure 8 here]

Case study 3: Test Panel 19

Test panel 19 is also the same size as panel Test 21 except this panel is simply supported on all 4 sides. Fig. 9(a) is the experimental failure pattern of the Test Panel 19 with the size 3750×2500×109 (Lawrence 1983) and four simply supported sides. Fig. 9(b) is the predicted failure pattern of the panel,

Test 19, which is plotted by matching cracking zones/cells between the base panel and the panel using the proposed technique.

The configuration and failure pattern of the base panel is based on the experiments of Panels Test 8 and Test 24 (Lawrence 1983), as shown in Fig. 10. These two panels are simply supported at all 4 edges. However, because the boundary types are symmetrical to their central horizontal and vertical lines, their ideal experimental patterns should also be symmetrical about these centre lines. Therefore Test panel 24 was favoured to be the most likely failure pattern for panels with four sides restrained and hence was used as the base panel.

Comparing Figs. 9(a) and 9(b), the predicted failure pattern, Fig 9(b), of the panel Test 19 is very close to its experimental result Fig 9(a). Once again this proves the validity of the proposed method.

[Insert Figure 9 here]

[Insert Figure 10 here]

DISCUSSION

The above results clearly show that failure patterns of panels are closely related to their boundary conditions and dimensions. The failure pattern of a panel is formed as a result of excessive tensile stress within a zone on the panel which causes the failure of that panel. The boundary conditions and panel dimensions dominate the location of the first cracked zone and the subsequent propagation of the crack to its neighbouring zones, until a full failure pattern is established.

The case studies used in this paper were selected carefully from published sources for which failure patterns recorded in the laboratory were available. The reason for this was to check the validity of the proposed CA method with the actual experimental results although different base panels were used in this process. The base panels were carefully chosen to have close similarity only in terms of boundary types. The sizes of all panels used in the case studies were different from the sizes of the base panels and still the proposed method proved to be valid and useful.

The results of the three case studies demonstrates that the CA provides an interesting alternative to conventional numerical methods that can reasonably accurately predict the failure pattern of masonry wall panels subject to lateral load. Further verification work and extending this methodology to predict failure load of masonry wall panels using the CA is under investigation by the authors. If this technique can be combined with the other IT techniques such as the artificial neural networks (Mathew et al.

1999), it can be expected that an artificial experimental environment for masonry panels may replace or reduce expensive masonry laboratory tests.

CONCLUSIONS

- The pattern matching techniques, using cellular automata, developed in this paper, can replace conventional finite element analysis and are able to predict the failure patterns of laterally loaded masonry wall panels with various boundary conditions.
- The boundary type and the variation in masonry properties at various locations within the panel, play a key role in the failure pattern of the masonry wall panels.
- The CA technique is capable of predicting the failure pattern of masonry wall panels subjected to lateral loading with reasonable accuracy without the help of any numerical techniques such as FEA.
- The techniques developed in this paper can be used as an inexpensive artificial experimental environment that can replace some of the physical tests for masonry panels, which can be very expensive.

ACNOWLEDGEMENT

The authors would like to thank the University of Plymouth for the financial support of this research. Thanks are also extended to Professor Lawrence, S.J. (1983), University of South Wales, Australia, for providing us with examples of wall panels to verify the validity of the methodologies proposed in this research.

REFERENCES

Baker, L.R. (1982). “A Principal Stress Failure Criterion for Brickwork in Bi-Axial Bending”. Proc. 6th IBMaC, Rome.

Brownjohn, J. M. W., Moyo, P., Omenzetter, P., and Lu, Y. (2003). “Assessment of highway bridge upgrading by testing and finite-element model updating.” *J. Bridge Eng.* 8(3), 162–172.

BSI, British Standards Institution (1992). *BS 5268: Part 1. Code of Practice for use of Masonry. Part 1. Structural Use of Unreinforced Masonry*. UK.

Castello, D. A., Stutz, L. T., and Rochinha, F. A., (2002). "A structural defect identification approach based on a continuum damage model." *Comput. Struct.* 80, 417–436.

Chong, V.L. (1993). The Behaviour of Laterally Loaded Masonry Panels with Openings. Thesis (PhD). University of Plymouth, UK.

"CSSA brickwork code." (1969). AS CA47-1969, Standards association of Australia, Sydney, Australia.

Edgell G. *The experimental results of laterally loaded masonry wall panels*. CERAM Building Technology.

Edward, R. (1989). *Exploring the geometry of nature – computer modelling of chaos, fractal, cellular automata and neural networks.* Blue Ridge Summit, PA: Windcrest Books.

Fishburn, C.C. (1961). Effect of Mortar Properties on Strength of Masonry. *National Bureau of Standards*, Monograph 36, Washington.

Fried, A.N. (1989) "Laterally Loaded Masonry Panels-The Significance of Analytical Methods and Material Properties". Thesis (Ph.D), Soutth Bank Polytechnic, London, UK.

Friswell, M. I., and Mottershead, J. E. (1995). *Finite element model updatingin structural dynamics*, Kluwer, New York.

Goles, Eric AND Mari'nez, Sevet. (1990). *Neural and Automata Networks: Dynamical Behavior and Applications*. Boston, Kluwer Academic Publishers.

Halpern, P. Sticks AND Stones (1989): A Guide to Structurally Dynamic Cellular Automata. *American Journal of Physics Teachers*, 57 (5).

Hemez, F. M., and Doebling, S. W. ~2001!. "Review and assessment of model updating for non-linear, transient dynamics." *Mech. Syst. SignalProcess.* 15(1), 45–74.

Hu, N., Wang, X., Fukunaga, H., Yao, Z. H., Zhang, H. X., and Wu, Z. S. (2001). "Damage assessment of structures using modal test data." *Int.J. Solids Struct.*, 38, 3111–3126.

Lawrence, S. J. (1983). "Behaviour of Brick Masonry Walls under Lateral Loading". Vols 1 and 2. Thesis (Ph.D.), University of South Wales, Australia.

Lawrence, S.J. and Lu, J.P. (1991). "An Elastic Analysis of Laterally Loaded Masonry Walls with Openings". International Symposium on Computer Methods in Structural Masonry. Swansea, UK.

Lee, J. S., Pande, G. N., Middleton, J. and Kralj. (1996). "Numerical Modelling of Brick Masonry Panels Subject to Lateral Loadings". *Computer and Structures,* Vol. 61, No. 4, 735-745.

Lourenco, P. B.(1997). "An Anisotropic Macro-Model for Masonry Plates and Shells: Implementation and Validtion." *Rep. 03.21.1.3.07*. University of Technology, Delft, The Netherlands.

Lourenco, P. B.(2000). "Anisotropic Softening Model for Masonry Plates and Shells". *Journal of Structural Engineering,* ASCE. Vol. 126, No. 9, 1008-1016.

Mathew, A., Kumar, B., Sinha, B. P. and Redreschi, R. F. (1999). "Analysis of Masonry Panel under Biaxial Bending Using ANNs and CBR". *Journal of Computing in Civil Engineering*. Vol. 13, No. 3. University of Edinburgh, UK.

Modak, S. V., Kundra, T. K., and Nakra, B. C. ~2002!. "Comparative study of model updating studies using simulated experimental data." *Comput. Struct.* 80, 437–447.

Rafiq, M. Y., Zhou, G. C. Bugmann, G. and Easterbrook, D. (2003). "Analysis of Brickwork Wall Panels Subjected to Lateral Loading Using Correctors". *Journal of Masonry International*, pp. 75-82, Vol 16, No 2, 2003.

Robert-Nicoud, Y. Raphael, B and Smith, I. F. C., (2005). "System Identification through Model Composition and Stochastic Search", Journal of Computing in Civil, Vol. 19, No, pp 239-247.

Rucker and Rudy. (1989). *CA Lab (Exploring Cellular Automata) – Rudy Rucker's Cellular Automata Laboratory*. Autodesk Inc., Sausalito, CA.

Sohn, H., and Law, K. H. (1997). "A Bayesian probabilistic approach for structural damage detection." *Earthquake Eng. Struct. Dyn.*, 26, 1259–1281.

Soschinske, K. A. (1997). *Cellular Automata Simulation of Resin Flow Through a Fiber Reinforcement*. UMI Dissertation Service.

Teughels, A., Maeck, J., and Roeck, G. (2002). "Damage assessment by FE model updating using damage functions." *Comput. Struct.* 80, 1869–1879.

West, H.W.H., Hodgkinson, H.R. and Webb, W.F. (1971). *The Resistance of Clay Brick Walls to Lateral Loading*. Technical Note, No. 176, The British Ceramic Research Association.

West, H.W.H., Hodgkinson, H.R. and Webb, W.F. (1971). *The Resistance of Clay Brick Walls to Lateral Loading*. Technical Note, No. 176, The British Ceramic Research Association.

Zhou, G. C. (2002). "Application of Stiffness/Strength Corrector and Cellular Automata in Predicting Response of Laterally Loaded Masonry Panels". Thesis (PhD), University of Plymouth, UK.

Zhou, G. C., Rafiq, M. Y. and Easterbrook, (2002). "A Different Approach to the Analysis of Brickwork Wall Panels Subjected to Lateral Loading". *6th International Masonry Conference*, London, UK.

Zhou, G. C., Rafiq, M. Y. and Easterbrook, D. (2002). "Application of Cellular Automata in Analysing Laterally Loaded Masonry Panels". *6th International Masonry Conference*, London, UK.

Zhou,G. C., Rafiq M. Y. Easterbrook, D. J., and Bugmann, G. (2003). "Application of cellular automata in modelling laterally loaded masonry panel boundary effects", Masonry International. Vol 16 No 3, pp 104-114. ISSN 0950-2289

http://www.tu-bs.de/institute/WiR/weimar/ZAscript/node2.html.

FIG. 1. Divided Zones of Panel SB01 Based on the Measured Laboratory Points.
FIG. 2. State values of Zones D2 and D8 along with their four neighbor zones
FIG. 3. The CA Model of Boundary Effect on Zones inside the Panel
FIG. 4. Eight possible for orientations of the CA cells for matching zone similarity
FIG. 5. Cellular Automata Neighborhoods von Neumann (1997)
FIG. 6**.** Failure Patterns of Panels SB01, SB05 and Test 29 as recorded in the laboratory
FIG. 7. Comparison of the experimental and predicted failure patterns of Panel Test 21
FIG. 8. Comparison of the experimental and predicted failure patterns of Test 16
FIG. 9. Comparison of the experimental and predicted failure patterns of Panel Test 19
FIG. 10**.** Failure Patterns of Panels Test 8 and Test 24 as recorded in the laboratory

Table 1. The State Values from Equations (2) and (3)
Table 2. The dimensions and boundary condition of wall panels used in case studies

Table 1.

		1	2	3	4	5	6	7	8	9	
		0	0	0	0	0	0	0	0	0	
A	0.2	**0.558**	**0.585**	**0.605**	**0.62**	**0.624**	**0.625**	**0.62**	**0.609**	**0.592**	0.4
B	0.2	**0.583**	**0.61**	**0.629**	**0.64**	**0.649**	**0.649**	**0.644**	**0.634**	**0.616**	0.4
C	0.2	**0.596**	**0.623**	**0.642**	**0.65**	**0.661**	**0.662**	**0.657**	**0.646**	**0.629**	0.4
D	0.2	**0.597**	**0.624**	**0.644**	**0.66**	**0.663**	**0.664**	**0.659**	**0.648**	**0.631**	0.4
		0.4	0.4	0.4	0.4	0.4	0.4	0.4	0.4	0.4	

Table 2: Details of panels used in case studies

Panel	Dimensions (mm)	Boundaries	Source
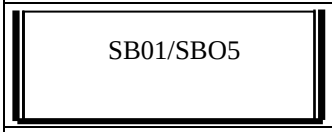 SB01/SBO5	5600 x 2475x102.5	Sides: Simply supported Base: Build-in Top: Free	University of Plymouth
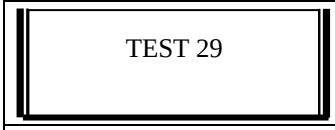 TEST 29	5600 x 2500 x 109	Three edges simply supported Top edge: Free	Lawrence University of New South Wales Australia
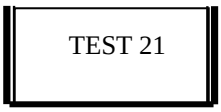 TEST 21	3750 x 2500 x 109	Three edges simply supported Top edge: Free	Lawrence University of New South Wales Australia
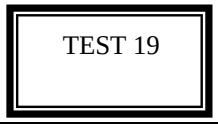 TEST 19	3750 x 2500 x 109	All edges simply supported	Lawrence University of New South Wales Australia
TEST 16	2500 x 2500 x 109	Three edges simply supported Top edge: Free	Lawrence University of New South Wales Australia
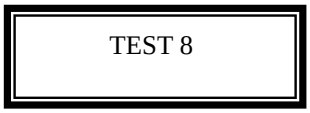 TEST 8	5000×2500×112	All edges simply supported	Lawrence University of New South Wales Australia
TEST 24	5000×2500×112	All edges simply supported	Lawrence University of New South Wales Australia

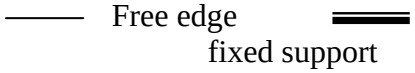 Free edge simple support

fixed support

NOTE: Panel SB05 had a damp proof course at its base

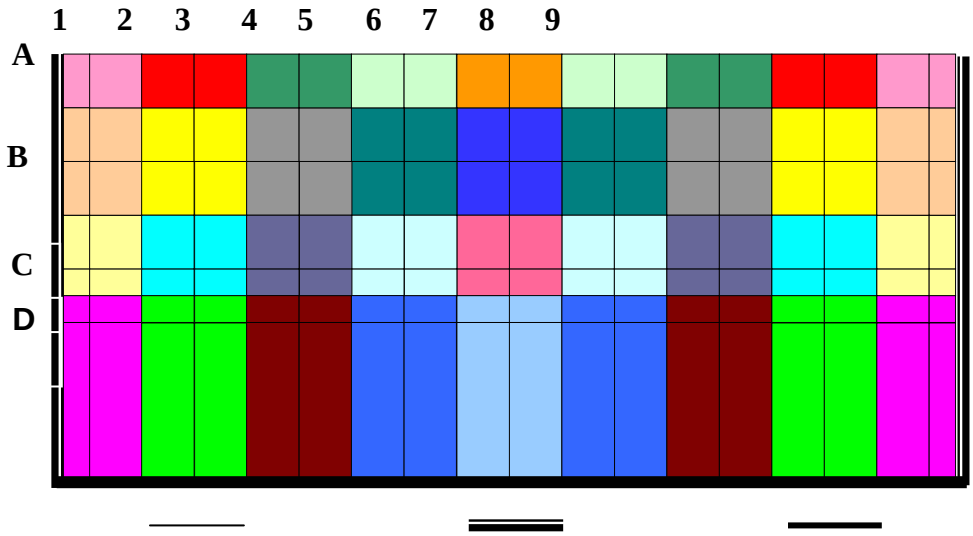

Free edge; simple support; fixed support

Note: The Measurement points are A1~A9, B1~B9, C1~C9 and D1~D9.

FIG. 1.

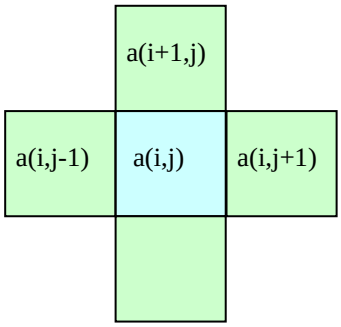

FIG. 2.

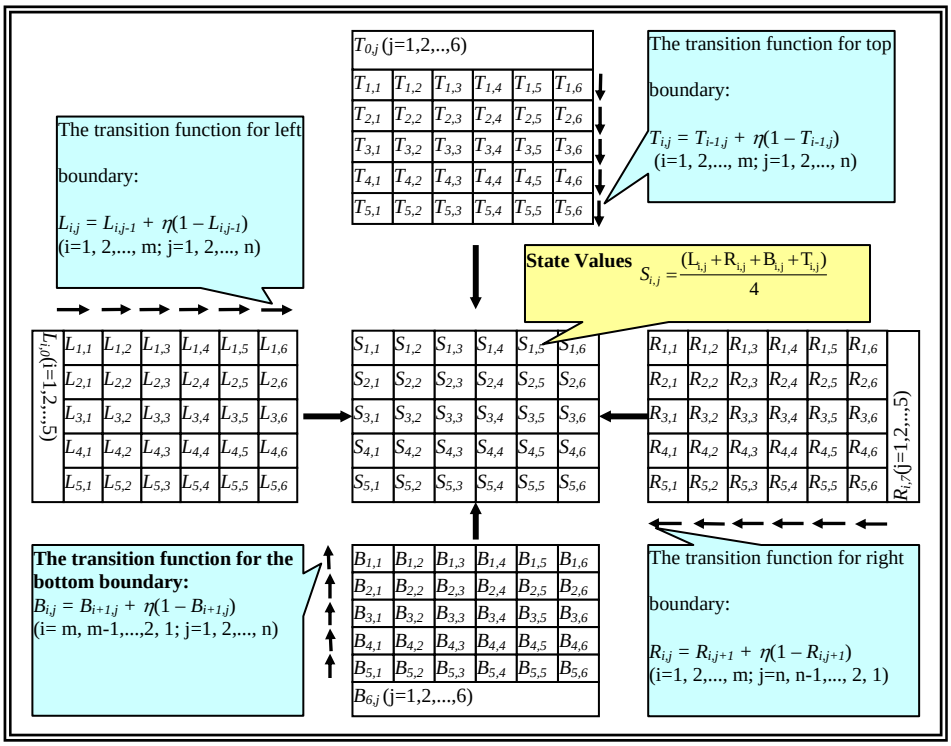
$T_{0,j}$ (j=1,2,..,6)
$T_{1,1}$ $T_{1,2}$ $T_{1,3}$ $T_{1,4}$ $T_{1,5}$ $T_{1,6}$
$T_{2,1}$ $T_{2,2}$ $T_{2,3}$ $T_{2,4}$ $T_{2,5}$ $T_{2,6}$
$T_{3,1}$ $T_{3,2}$ $T_{3,3}$ $T_{3,4}$ $T_{3,5}$ $T_{3,6}$
$T_{4,1}$ $T_{4,2}$ $T_{4,3}$ $T_{4,4}$ $T_{4,5}$ $T_{4,6}$
$T_{5,1}$ $T_{5,2}$ $T_{5,3}$ $T_{5,4}$ $T_{5,5}$ $T_{5,6}$
The transition function for top boundary:
$T_{i,j} = T_{i-1,j} + \eta(1 - T_{i-1,j})$
(i=1, 2,..., m; j=1, 2,..., n)
The transition function for left boundary:
$L_{i,j} = L_{i,j-1} + \eta(1 - L_{i,j-1})$
(i=1, 2,..., m; j=1, 2,..., n)
State Values $S_{i,j} = \frac{(L_{i,j} + R_{i,j} + B_{i,j} + T_{i,j})}{4}$
$L_{i,j}$(i=1,2,..,5)
$L_{1,1}$ $L_{1,2}$ $L_{1,3}$ $L_{1,4}$ $L_{1,5}$ $L_{1,6}$
$L_{2,1}$ $L_{2,2}$ $L_{2,3}$ $L_{2,4}$ $L_{2,5}$ $L_{2,6}$
$L_{3,1}$ $L_{3,2}$ $L_{3,3}$ $L_{3,4}$ $L_{3,5}$ $L_{3,6}$
$L_{4,1}$ $L_{4,2}$ $L_{4,3}$ $L_{4,4}$ $L_{4,5}$ $L_{4,6}$
$L_{5,1}$ $L_{5,2}$ $L_{5,3}$ $L_{5,4}$ $L_{5,5}$ $L_{5,6}$
$S_{1,1}$ $S_{1,2}$ $S_{1,3}$ $S_{1,4}$ $S_{1,5}$ $S_{1,6}$
$S_{2,1}$ $S_{2,2}$ $S_{2,3}$ $S_{2,4}$ $S_{2,5}$ $S_{2,6}$
$S_{3,1}$ $S_{3,2}$ $S_{3,3}$ $S_{3,4}$ $S_{3,5}$ $S_{3,6}$
$S_{4,1}$ $S_{4,2}$ $S_{4,3}$ $S_{4,4}$ $S_{4,5}$ $S_{4,6}$
$S_{5,1}$ $S_{5,2}$ $S_{5,3}$ $S_{5,4}$ $S_{5,5}$ $S_{5,6}$
$R_{1,1}$ $R_{1,2}$ $R_{1,3}$ $R_{1,4}$ $R_{1,5}$ $R_{1,6}$
$R_{2,1}$ $R_{2,2}$ $R_{2,3}$ $R_{2,4}$ $R_{2,5}$ $R_{2,6}$
$R_{3,1}$ $R_{3,2}$ $R_{3,3}$ $R_{3,4}$ $R_{3,5}$ $R_{3,6}$
$R_{4,1}$ $R_{4,2}$ $R_{4,3}$ $R_{4,4}$ $R_{4,5}$ $R_{4,6}$
$R_{5,1}$ $R_{5,2}$ $R_{5,3}$ $R_{5,4}$ $R_{5,5}$ $R_{5,6}$
$R_{i,7}$(i=1,2,..,5)
The transition function for the bottom boundary:
$B_{i,j} = B_{i+1,j} + \eta(1 - B_{i+1,j})$
(i= m, m-1,...,2, 1; j=1, 2,..., n)
$B_{1,1}$ $B_{1,2}$ $B_{1,3}$ $B_{1,4}$ $B_{1,5}$ $B_{1,6}$
$B_{2,1}$ $B_{2,2}$ $B_{2,3}$ $B_{2,4}$ $B_{2,5}$ $B_{2,6}$
$B_{3,1}$ $B_{3,2}$ $B_{3,3}$ $B_{3,4}$ $B_{3,5}$ $B_{3,6}$
$B_{4,1}$ $B_{4,2}$ $B_{4,3}$ $B_{4,4}$ $B_{4,5}$ $B_{4,6}$
$B_{5,1}$ $B_{5,2}$ $B_{5,3}$ $B_{5,4}$ $B_{5,5}$ $B_{5,6}$
$B_{6,j}$ (j=1,2,...,6)
The transition function for right boundary:
$R_{i,j} = R_{i,j+1} + \eta(1 - R_{i,j+1})$
(i=1, 2,..., m; j=n, n-1,..., 2, 1)

Fig 3

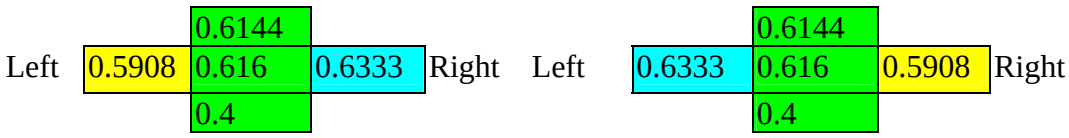

(a) Zone D2 (b) Zone D8

Fig. 4

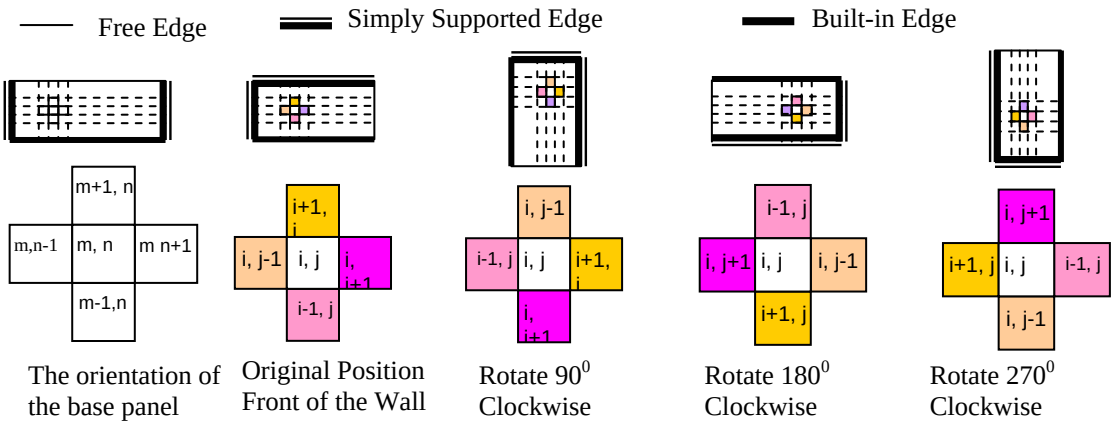

(a): Four possible for orientations facing the front of the wall

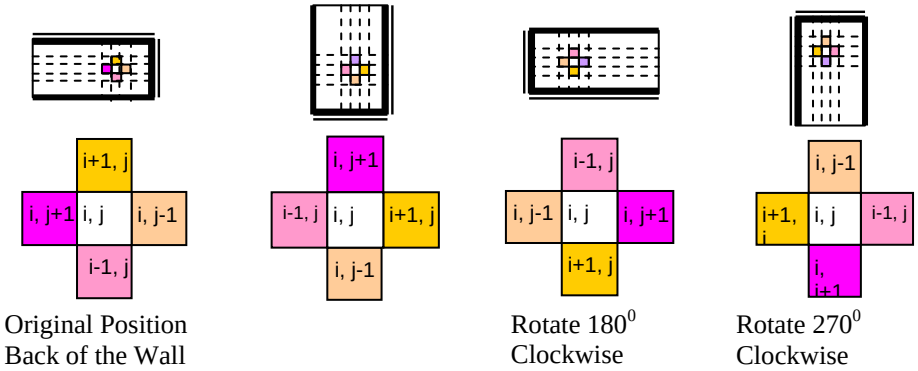

(b): Four possible for orientations facing the back of the wall

Fig. 5.

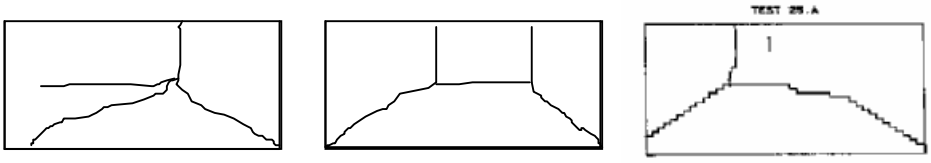

5600×2475×102.5 (b) Pa 5600×2475×102.5 Panel T 5600×2500×109

FIG. 6.

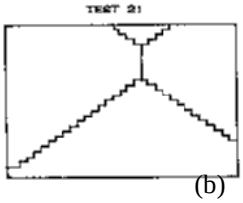

(a)

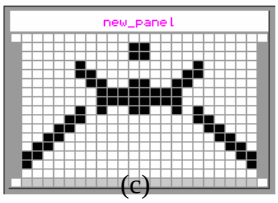

(b)

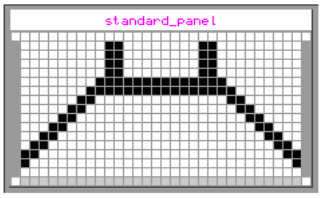

(c)

(a) The experimental failure pattern of Panel Test 21;
(b) The predicted failure pattern of Panel Test 21 by the CA technique;
(c) The failure pattern of the base panel based on the experimental records of standard panels.

FIG. 7.

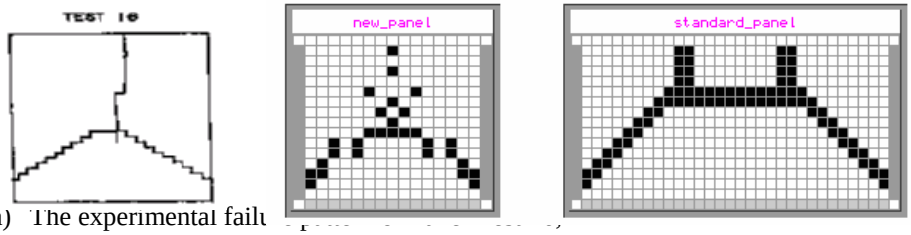

(a) The experimental failu
(b) The predicted failure pattern of Panel Test 16 by the CA technique;
(c) The failure pattern of the base panel based on the experimental records of standard panels.

FIG. 8.

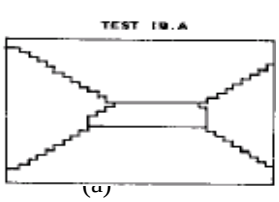

(a)

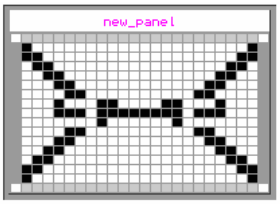

(b)

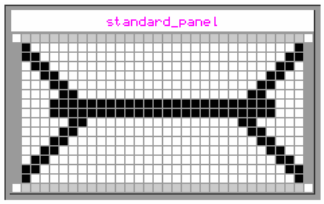

(c)

(a) The experimental failure pattern of Panel Test 19;
(b) The predicted failure pattern of Panel Test 19 by the CA technique;
(c) The failure pattern of the base panel based on the experimental records of standard panels.

FIG. 9.

Test 8

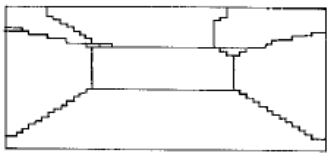

5000×2500×112

(a) Failure Pattern of Panel Test 8

Test 24

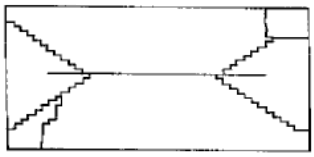

5000×2500×112

(b) Failure Pattern of Panel Test 24

FIG. 10